(23) Richards, R. W.; Thomason, J. L. *Polymer* **1981**, *22*, 581.
(24) Cebula, D. J.; Ottewill, R. H.; Ralston, J. *J. Chem. Soc., Faraday Trans. 1* **1981**, *77*, 2585.
(25) Ottewill, R. H. "Colloidal Dispersions"; Goodwin, J. W., Ed.; Royal Society of Chemistry: London, 1982; pp 197-217.
(26) Ottewill, R. H. "Science and Technology of Polymer Colloids"; Poehlein, G. W., Ottewill, R. H., Goodwin, J. W., Eds.; Martinus Nijhoff Publishers: Boston, 1983; NATO ASI Series, Vol. II, pp 503-522.
(27) Guinier, A.; Fournet, G. "Small-Angle Scattering of X-Rays"; Wiley: New York, 1955.
(28) Zernike, F.; Prins, J. A. *Z. Phys.* **1927**, *41*, 184.
(29) Debye, P. *Phys. Z.* **1927**, *28*, 135.
(30) Born, M.; Green, H. S. *Proc. R. Soc. London, Ser. A* **1946**, *188*, 10.
(31) Fournet, P. G. *Acta Crystallogr.* **1951**, *4*, 293.
(32) Rodriguez, A. E. *Proc. R. Soc. London, Ser. A* **1949**, *196*, 73.
(33) Barker, J. A.; Henderson, D. *Rev. Mod. Phys.* **1976**, *43*, 587.
(34) Ornstein, L. S.; Zernike, F. *Proc. Akad. Sci. Amsterdam* **1914**, *17*, 793.
(35) Percus, J. K.; Yevick, G. J. *Phys. Rev.* **1958**, *110*, 1.
(36) Wertheim, M. S. *Phys. Rev. Lett.* **1963**, *10*, 321.
(37) Thiele, E. *J. Chem. Phys.* **1963**, *39*, 474.
(38) Ashcroft, N. W.; Lekner, J. *Phys. Rev.* **1966**, *145*, 83.
(39) Kaler, E. N.; Bennett, K. E.; Davis, H. T.; Scriven, L. E. *J. Chem. Phys.* **1983**, *79* (11), 5673.
(40) Bates, F. S.; Cohen, R. E.; Berney, C. V. *Macromolecules* **1982**, *15*, 589.
(41) Vrij, A. *J. Chem. Phys.* **1979**, *71* (8), 3267.
(42) van Beurten, P.; Vrij, A. *J. Chem. Phys.* **1981**, *74* (5), 2744.
(43) Helfand, E.; Wasserman, Z. *Macromolecules* **1978**, *11*, 960.
(44) Roe, R. J.; Fishkis, M.; Chang, J. C. *Macromolecules* **1981**, *14*, 1091.
(45) Meier, D. J. *Polym. Prepr., Am. Chem. Soc., Div. Polym. Chem.* **1977**, *18*, 340.
(46) Roe, R.-J.; Zin, W. C.; Fishkis, M. IUPAC Proceedings 1982, p 662.
(47) Hosemann, R.; Bagchi, S. W. "Direct Analysis of Diffraction by Matter"; North-Holland Publishing Co. (Amsterdam) and Interscience (New York), 1962.
(48) Meier, D. J. *J. Phys. Chem.* **1967**, *71* (6), 1861.
(49) Hesselink, F. Th.; Vrij, A.; Overbeek, J. Th. G. *J. Phys. Chem.* **1971**, *75* (14), 2094.
(50) Klein, J. *Nature (London)* **1980**, *288*, 248.
(51) Klein, J. *Faraday Trans. 1* **1983**, *79*, 99.
(52) Israelachvili, J. N.; Tirrell, M.; Klein, J.; Almog, Y. *Macromolecules* **1984**, *17*, 204.
(53) de Gennes, P. G. *Macromolecules* **1980**, *13*, 1069.

A Highly Convergent Algorithm for Computing the Orientation Distribution Functions of Rodlike Particles

Judith Herzfeld,*† Alan E. Berger,‡ and John W. Wingate‡

Department of Physiology and Biophysics, Harvard Medical School, Boston, Massachusetts 02115, and Applied Mathematics Branch, Naval Surface Weapons Center, Silver Spring, Maryland 20910. *Received December 13, 1983*

ABSTRACT: A salient difficulty in describing the phase behavior of rodlike particles with large axial ratios or high packing densities has been the solution of the nonlinear integral equation for the orientation distribution function. Approximations that do well for small axial ratios and low packing densities become increasingly unsatisfactory as the axial ratio or the packing density increases. In this report, we demonstrate that solutions of high accuracy may be obtained relatively efficiently by an iterative procedure that converges particularly rapidly for systems with high packing densities and large axial ratios. We show that, for polydisperse as well as monodisperse systems, each iteration moves in a direction of locally decreasing free energy. Although it does not necessarily follow that the net free energy change in a discrete step will be negative, all cases examined thus far generate successive distribution functions with monotonically decreasing free energy.

Introduction

Generalized van der Waals theory has been used with notable success to describe the structure and dynamics of the dense phases of nonassociated systems. (See Chandler et al.[1] for a recent review.) In these materials, intermolecular potentials may be satisfactorily separated into short-ranged repulsions treated as hard-core packing constraints and long-ranged interactions treated in terms of a mean field. One of the limitations in applying this theory to nematic systems has been the difficulty of accurately solving the relevant equations for the particle orientation distribution. In this paper we present an efficient iterative procedure that generates successive particle orientation distributions with monotonically decreasing free energy and converges rapidly to local free energy minima. The procedure also allows for estimation and reduction of the numerical error in the properties calculated from the distribution functions.

According to the van der Waals description, the free energy of N monodisperse rodlike particles with orientations $\Omega = (\theta,\phi)$ ($0 \leq \theta \leq \pi$ and $0 \leq \phi \leq 2\pi$) given by the distribution function $f(\Omega)$ is

$$F\{f(\Omega)\}/NkT = A + \int f(\Omega) \ln f(\Omega)\, d\Omega + \frac{B}{2}\int\int f(\Omega_1)f(\Omega_2) \sin(\gamma_{12})\, d\Omega_1\, d\Omega_2 + \frac{1}{2kT}\int f(\Omega)\psi(\Omega)\, d\Omega \quad (1)$$

where $d\Omega = (1/4\pi) \sin\theta\, d\theta\, d\phi$, γ_{12} is the angle between the axis of a rod with orientation Ω_1 and the axis of a rod with orientation Ω_2, the coefficients A and B are functions of particle asymmetry and particle volume fraction that depend on the model employed for the hard-core reference system, and $\psi(\Omega)$ is the mean field created by long-ranged interparticle forces.[2] In this equation the contributions of orientational entropy (favoring random orientation), translation entropy (favoring alignment), and internal energy (generally also favoring alignment) are represented by the seond, third, and fourth terms, respectively.

Considerations of self-consistency[3] and pair-volume exclusion[4] are satisfied by a mean field of the form

$$\psi(\Omega_1) = \rho\int U(\gamma_{12})f(\Omega_2)\, d\Omega_2 \quad (2)$$

where ρ is the particle number density and $U(\gamma_{12})$ depends

† Harvard Medical School.
‡ Naval Surface Weapons Center.

0024-9297/84/2217-1718$01.50/0

on the shape of the particles and the nature of the long-ranged interactions between them. Thus, the free energy may be expressed as

$$F\{f(\Omega)\}/NkT = A + \int f(\Omega) \ln f(\Omega)\, d\Omega + \frac{B}{2}\int\int f(\Omega_1)f(\Omega_2)W(\gamma_{12})\, d\Omega_1\, d\Omega_2 \quad (3)$$

where

$$W(\gamma_{12}) = \sin(\gamma_{12}) + \frac{\rho}{kTB}U(\gamma_{12}) \quad (4)$$

The most probable orientation distribution is the one that minimizes this free energy subject to the normalization constraint

$$\int f(\Omega)\, d\Omega = 1 \quad (5)$$

Previous Approaches

Several workers have approached this problem by choosing a parametrized form for the distribution function and minimizing the free energy function with respect to the parameters. Lasher[5] expanded the cylindrically symmetric distribution function in Legendre polynomials of even order

$$f(\Omega) = 1 + \sum_{m=2,2}^{M} (2m+1)\eta_m P_m(\cos\theta) \quad (6a)$$

where

$$\eta_m = \int f(\Omega) P_m(\cos\theta)\, d\Omega \quad (6b)$$

evaluated the free energy by Gaussian integration and minimized with respect to the coefficients of the series by Newton's method. With enough terms, the result is accurate; however, the series is rather slowly converging for large values of B (i.e., high packing densities or large axial ratios). This is because eq 6 requires progressively more terms to express narrower orientation distributions.

Approximate solutions may be obtained with a closed-form distribution function. Onsager[6] and Baron and Gelbart[7] assumed a cylindrically symmetric distribution function of the type

$$f(\Omega) = \frac{\cosh(\alpha\cos\theta)}{\int \cosh(\alpha\cos\theta)\, d\Omega} \quad (7)$$

and minimized the free energy with respect to the single parameter α. This procedure is relatively simple, but it tends to exaggerate the orientational order due to the steepness of the distribution function at the pole ($\theta = 0$).

Alben[8] and Cotter[9] have taken the alternative approach of approximating the free energy itself by an analytically minimizable expression. By approximating $W(\gamma)$ in eq 3 with the series

$$W(\gamma) = \sum_{m=0,2}^{M} w_m P_m(\cos\gamma) \quad (8)$$

γ_{12} can be eliminated from the free energy expression for cylindrically symmetric distribution functions, with the result that

$$F\{f(\Omega)\}/NkT = A + \int f(\Omega)\ln f(\Omega)\, d\Omega + \frac{B}{2}\sum_{m=0,2}^{M} w_m\eta_m^2 \quad (9)$$

(see, for example, ref 10). According to the calculus of variations, the extrema of this free energy expression satisfy the equation

$$0 = \ln f(\Omega) + B\sum_{m=0,2}^{M} w_m\eta_m P_m(\cos\theta) + \lambda \quad (10)$$

where λ is the Lagrange multiplier determined by the constraint in eq 5. Thus

$$f(\Omega) = \frac{\exp[-B\sum_{m=2,2}^{M} w_m\eta_m P_m(\cos\theta)]}{\int \exp[-B\sum_{m=2,2}^{M} w_m\eta_m P_m(\cos\theta')]\, d\Omega'} \quad (11)$$

where self-consistency requires that

$$\eta_m = \int P_m(\cos\theta)\exp[-B\sum_{m'=2,2}^{M} w_{m'}\eta_{m'}P_{m'}(\cos\theta)]\, d\Omega \Big/ \int \exp[-B\sum_{m'=2,2}^{M} w_{m'}\eta_{m'}P_{m'}(\cos\theta)]\, d\Omega \quad (12)$$

Cotter[9] and Alben[8] set $M = 2$ so that eq 12 comprises a single equation for η_2. Although the error is less for Cotter's choice of w_2 than for Alben's, both approximations do poorly at high packing densities and high axial ratios.[11]

More generally, if we take

$$w_m = \frac{2m+1}{2}\int_0^\pi W(\gamma)P_m(\cos\gamma)\sin\gamma\, d\gamma \quad (13)$$

and choose M large enough, eq 8 is exact and eq 12 involves $M/2$ relationships in $M/2$ unknowns for which the isotropic state ($\eta_m = 0$ for $m \geq 2$) is always a solution. Kayser and Raveché[12] have obtained the stable anisotropic solutions for these equations by iteration. Gelbart and Gelbart[4] have pointed out that even though the w_m are generaly not such as to produce rapid convergence in the sum of eq 8, M may be taken to be 2 or 4 with good accuracy if the η_m decrease quickly enough to ensure rapid convergence of the sums in eq 9–12. However, as discussed in connection with eq 6 above, this is not the case for large values of B. When B is large, the orientation distribution function is strongly peaked at the pole ($\theta = 0$) and the accuracy of $W(\gamma)$ at $\gamma \sim 0$ becomes important. Even for $M = 24$ and $U = 0$, evaluation of $W(\gamma)$ by eq 8, using the coefficients given by eq 13, leads to a value of 0.039 instead of 0 at $\gamma = 0$ (see, for example, ref 13).

The Algorithm

If the calculus of variations is applied directly to the original free energy expression in eq 3, the extrema of the free energy are found to be solutions of the nonlinear integral equation

$$0 = \ln f(\Omega_1) + B\int f(\Omega_2)W(\gamma_{12})\, d\Omega_2 + \lambda \quad (14)$$

where λ is the Lagrange multiplier determined by the constraint given in eq 5. Thus properly normalized,

$$f(\Omega_1) = \frac{\exp\left[-B\int f(\Omega_2)W(\gamma_{12})\, d\Omega_2\right]}{\int \exp\left[-B\int f(\Omega_2)W(\gamma_{23})\, d\Omega_2\right] d\Omega_3} \quad (15)$$

The form of eq 15 suggests the possibility of obtaining a solution by iterating from right to left, i.e., by repeatedly using the formula

$$f^{(n+1)}(\Omega_1) = \frac{\exp\left[-B\int f^{(n)}(\Omega_2)W(\gamma_{12})\, d\Omega_2\right]}{\int \exp\left[-B\int f^{(n)}(\Omega_2)W(\gamma_{23})\, d\Omega_2\right] d\Omega_3} \quad (16)$$

This is exactly analogous to the procedure used by Kayser and Raveché[12] to solve eq 12. Clearly, if the iteration

converges, so that $f^{(n+1)}(\Omega) = f^{(n)}(\Omega)$ for $n \geq N$, then $f^{(N)}(\Omega)$ is a solution to eq 15. Since each iterate satisfies eq 5

$$\left.\frac{\partial F\{f^{(n)}(\Omega) + \delta[f^{(n+1)}(\Omega) - f^{(n)}(\Omega)]\}/NkT}{\partial\delta}\right|_{\delta=0} =$$
$$\int [f^{(n+1)}(\Omega) - f^{(n)}(\Omega)] \ln f^{(n)}(\Omega)\, d\Omega +$$
$$B\int\int [f^{(n+1)}(\Omega_1) - f^{(n)}(\Omega_1)] f^{(n)}(\Omega_2) W(\gamma_{12})\, d\Omega_1\, d\Omega_2$$
$$= \int [f^{(n+1)}(\Omega) - f^{(n)}(\Omega)] \ln f^{(n)}(\Omega)\, d\Omega -$$
$$\int [f^{(n+1)}(\Omega) - f^{(n)}(\Omega)] \ln f^{(n+1)}(\Omega)\, d\Omega =$$
$$-\int [f^{(n+1)}(\Omega) - f^{(n)}(\Omega)][\ln f^{(n+1)}(\Omega) - \ln f^{(n)}(\Omega)]\, d\Omega < 0 \quad (17)$$

unless $f^{(n+1)}(\Omega) = f^{(n)}(\Omega)$. Thus, we know that each iteration moves in a direction of locally decreasing free energy in the sense that, when $f^{(n+1)}(\Omega) \neq f^{(n)}(\Omega)$, $F\{f^{(n)}(\Omega) + \delta[f^{(n+1)}(\Omega) - f^{(n)}(\Omega)]\} < F\{f^{(n)}(\Omega)\}$ for small positive δ. However, it is not clear that the net change in free energy in a discrete step ($\delta = 1$) is necessarily negative or that a series of such steps will converge.

For a mixture of several different types, σ, of rodlike particles, the free energy is given by an equation of the form

$$F\{f_\sigma(\Omega)\}/NkT = A + \sum_\sigma y_\sigma \int f_\sigma(\Omega) \ln f_\sigma(\Omega)\, d\Omega +$$
$$\sum_\sigma\sum_{\sigma'} y_\sigma y_{\sigma'} \frac{B^{\sigma\sigma'}}{2} \int\int f_\sigma(\Omega_1) f_{\sigma'}(\Omega_2) W^{\sigma\sigma'}(\gamma_{12})\, d\Omega_1\, d\Omega_2 \quad (18)$$

where each $f_\sigma(\Omega)$ is subject to the normalization constraint in eq 5, y_σ is the number fraction of particles of type σ, $B^{\sigma\sigma'} = B^{\sigma'\sigma}$, and $W^{\sigma\sigma'} = W^{\sigma'\sigma}$ (see ref 14). The corresponding analogues of eq 14–16 can be developed for this polydisperse system, and the result corresponding to eq 17 also remains valid.

Numerical Implementation

The iteration of eq 16 for monodisperse rods was implemented as follows. For any functions $g(\Omega)$ and $G(\gamma_{12}) = G(\arccos[\sin\theta_1 \sin\theta_2 \cos(\phi_1 - \phi_2) + \cos\theta_1 \cos\theta_2]) = G(\theta_1,\theta_2,\phi_1 - \phi_2)$ let

$$\langle g(\Omega)\rangle \equiv \int f(\Omega) g(\Omega)\, d\Omega \quad (19)$$

and

$$\langle\langle G(\gamma)\rangle\rangle \equiv \int\int f(\Omega_1) f(\Omega_2) G(\gamma_{12})\, d\Omega_1\, d\Omega_2 \quad (20)$$

Then, for cylindrically symmetric functions, $g(\Omega) = g(\theta) = g(\pi - \theta)$ and $f(\Omega) = f(\theta) = f(\pi - \theta)$,

$$\langle g(\theta)\rangle = \int_0^{\pi/2} f(\theta) g(\theta) \sin\theta\, d\theta \quad (21)$$

and, when $G(\pi - \gamma_{12}) = G(\gamma_{12})$,

$$\langle\langle G(\gamma)\rangle\rangle = \int_0^{\pi/2}\int_0^{\pi/2} f(\theta_1) f(\theta_2) \bar{G}(\theta_1,\theta_2) \sin\theta_1 \sin\theta_2\, d\theta_1\, d\theta_2 \quad (22a)$$

where

$$\bar{G}(\theta_1,\theta_2) = \frac{1}{2\pi}\int_0^{2\pi} \frac{1}{2\pi}\int_0^{2\pi} G(\gamma_{12})\, d\phi_1\, d\phi_2 =$$
$$\frac{1}{2\pi}\int_0^{2\pi} G(\theta_1,\theta_2,\phi_1 - \phi_2)\, d(\phi_1 - \phi_2) \quad (22b)$$

These integrals were discretized with the following trapezoidal quadrature formula. Positive intergers J and J_ϕ where chosen determining subinterval lengths, $\Delta\theta = \pi/(2J)$ and $\Delta\phi = 2\pi/J_\phi$, and grid points, $\theta_i = i(\Delta\theta)$ ($i = 0, 1, ..., J$) and $\phi_k = k(\Delta\phi)$ ($k = 0, 1, ..., J_\phi$). Letting f_i denote the numerical value for $f(\theta_i)$ and defining the trapezoidal quadrature weights $t_i = 1$ for $i = 1, ..., J-1$, $t_0 = t_J = {}^1/_2$, $\tilde{t}_k = 1$ for $k = 1, ..., J_\phi - 1$, and $\tilde{t}_0 = \tilde{t}_{J_\phi} = {}^1/_2$,

$$\langle g(\theta)\rangle \cong (\Delta\theta)\sum_{i=0}^{J} t_i f_i g(\theta_i) \sin\theta_i \quad (23)$$

and

$$\langle\langle G(\gamma)\rangle\rangle \cong (\Delta\theta)^2 \sum_{i=0}^{J}\sum_{j=0}^{J} t_i t_j f_i f_j \bar{G}(\theta_i,\theta_j) \sin\theta_i \sin\theta_j \quad (24a)$$

where

$$\bar{G}(\theta_i,\theta_j) \cong \frac{1}{2\pi}(\Delta\phi)\sum_{k=0}^{J_\phi} \tilde{t}_k G(\theta_i,\theta_j,\phi_k) \quad (24b)$$

The free energy, discretized in this manner and subject to the discretized normalization constraint, has a positive global minimizing distribution f_i that converges for some sequence J and $J_\phi \to \infty$ to a positive global minimum $f(\Omega)$ of the original free energy, subject to the original normalization constraint; when the free energy has a unique global minimizing distribution, then f_i converges to it for every sequence of J and $J_\phi \to \infty$.[15]

The Lagrange multiplier equation for the extrema of the discretized free energy functional, subject to the discretized normalization condition, is precisely the trapezoidal quadrature discretization of eq 14 and hence eq 15. Writing this in iterative form, corresponding to eq 16, and noting that $\sin\theta_0 = 0$ and $W(\theta_1,\theta_2,\phi_0) = W(\theta_1,\theta_2,\phi_{J_\phi})$, one obtains for $1 \leq i \leq J$

$$f_i^{n+1} = \tilde{f}_i^{n+1}/[(\Delta\theta)\sum_{l=1}^{J} t_l \tilde{f}_l^{n+1} \sin\theta_l] \quad (25a)$$

where

$$\tilde{f}_i^{n+1} = \exp[-B(\Delta\theta)\sum_{j=1}^{J} \bar{W}(\theta_i,\theta_j) f_j^n t_j \sin\theta_j] \quad (25b)$$

and

$$\bar{W}(\theta_i,\theta_j) = \frac{1}{2\pi}(\Delta\phi)\sum_{k=1}^{J_\phi} W(\theta_i,\theta_j,\phi_k) \quad (25c)$$

In this iteration, each step moves in a direction of local decrease in the discretized free energy according to the discretized analogue of eq 17. For the numerical implementation, J_ϕ was set equal to 2048 and the values $\bar{W}(i\pi/128, j\pi/128)$, $1 \leq i, j \leq 64$, were calculated once and permanently stored. This permitted execution of the iterations without recomputing $\bar{W}(\theta_i,\theta_j)$ for J any power of 2 not larger than 64. For any set of values f_i, $1 \leq i \leq J$, the value f_0 approximating $f(0)$ was defined to be the value at $\theta = 0$ of the quadratic polynomial $q(\theta)$ satisfying $q(\theta_i) = f_i$ for $i = 1, 2, 3$.

The criterion for determining when the iteration had converged was heuristically defined as follows. Let H denote the mapping function defined by eq 25 which takes a set of values f_i^n into f_i^{n+1} and assume for a given set of starting values f_i^0 that the iteration converges to a set of values f_i satisfying $f_i = H(f_i)$. For any set of values f_i^n define the error as

$$e_n = ||f_i - f_i^n||/||f_i|| \quad (26a)$$

where for any set of values $\tilde{f}_i$

$$||\tilde{f}_i|| \equiv \max_{1\leq i\leq J} |\tilde{f}_i| \quad (26b)$$

Table I
Properties of the Axial Solutions of Eq 15 for the Hard-Core Reference System ($U = 0$)[a]

B	J	f(0)	L	$\frac{\pi}{4}-\langle\langle\sin\gamma\rangle\rangle$	$\langle\ln f(\theta)\rangle$	$\langle P_2(\cos\theta)\rangle$	$\langle P_4(\cos\theta)\rangle$	Error
8.88	64	.998	.87	2.223E-07	5.049E-05	-3.884E-04	-5.616E-05	-------
8.89	64	5.41	.97	1.020E-01	4.015E-01	4.499E-01	1.511E-01	-------
8.90	RE	5.77	.95	1.118E-01	5.047E-01	4.706E-01	1.654E-01	-------
9.00	RE	7.16	.90	1.476E-01	6.651E-01	5.381E-01	2.175E-01	2: 3RD
9.10	RE	8.15	.86	1.712E-01	7.718E-01	5.776E-01	2.520E-01	1: 3RD
9.20	RE	9.00	.82	1.903E-01	8.594E-01	6.073E-01	2.803E-01	4: 4TH
9.30	RE	9.77	.79	2.068E-01	9.360E-01	6.315E-01	3.047E-01	4: 4TH
9.40	RE	10.5	.77	2.216E-01	1.005E+00	6.523E-01	3.268E-01	4: 4TH
9.50	RE	11.2	.74	2.351E-01	1.069E+00	6.703E-01	3.468E-01	3: 4TH
9.60	RE	11.9	.72	2.474E-01	1.128E+00	6.862E-01	3.653E-01	3: 4TH
9.70	RE	12.5	.70	2.589E-01	1.183E+00	7.006E-01	3.827E-01	3: 4TH
9.80	RE	13.2	.68	2.695E-01	1.234E+00	7.135E-01	3.988E-01	3: 4TH
9.90	RE	13.8	.67	2.795E-01	1.283E+00	7.254E-01	4.141E-01	3: 4TH
10.00	RE	14.4	.65	2.890E-01	1.332E+00	7.364E-01	4.286E-01	3: 4TH
10.10	RE	15.1	.64	2.979E-01	1.377E+00	7.465E-01	4.424E-01	3: 4TH
10.20	RE	15.7	.62	3.064E-01	1.419E+00	7.557E-01	4.556E-01	3: 4TH
10.30	RE	16.3	.61	3.145E-01	1.460E+00	7.644E-01	4.681E-01	3: 4TH
10.40	RE	16.9	.60	3.222E-01	1.500E+00	7.726E-01	4.801E-01	3: 4TH
10.50	RE	17.5	.59	3.296E-01	1.538E+00	7.802E-01	4.916E-01	3: 4TH
10.60	RE	18.1	.58	3.366E-01	1.576E+00	7.873E-01	5.026E-01	3: 4TH
10.70	RE	18.7	.57	3.434E-01	1.612E+00	7.941E-01	5.132E-01	3: 4TH
10.80	RE	19.3	.56	3.499E-01	1.646E+00	8.003E-01	5.234E-01	3: 4TH
10.90	RE	19.9	.55	3.561E-01	1.680E+00	8.063E-01	5.332E-01	3: 4TH
11.00	RE	20.5	.54	3.621E-01	1.713E+00	8.120E-01	5.427E-01	3: 4TH
11.10	RE	21.1	.53	3.679E-01	1.745E+00	8.174E-01	5.518E-01	3: 4TH
11.20	RE	21.7	.53	3.735E-01	1.776E+00	8.225E-01	5.607E-01	3: 4TH
11.30	RE	22.3	.52	3.788E-01	1.806E+00	8.273E-01	5.692E-01	3: 4TH
11.40	RE	22.9	.51	3.841E-01	1.836E+00	8.320E-01	5.775E-01	3: 4TH
11.50	RE	23.5	.51	3.891E-01	1.865E+00	8.364E-01	5.855E-01	3: 4TH
11.60	RE	24.1	.50	3.940E-01	1.893E+00	8.406E-01	5.932E-01	3: 4TH
11.70	RE	24.7	.49	3.987E-01	1.920E+00	8.446E-01	6.007E-01	3: 4TH
11.80	RE	25.3	.49	4.033E-01	1.947E+00	8.483E-01	6.080E-01	3: 4TH
11.90	RE	25.9	.48	4.077E-01	1.974E+00	8.520E-01	6.151E-01	3: 4TH
12.00	RE	26.6	.48	4.120E-01	1.999E+00	8.557E-01	6.219E-01	3: 4TH
12.10	RE	27.2	.48	4.162E-01	2.026E+00	8.589E-01	6.286E-01	3: 4TH
12.20	RE	27.8	.47	4.203E-01	2.049E+00	8.622E-01	6.351E-01	3: 4TH
12.30	RE	28.4	.47	4.242E-01	2.075E+00	8.653E-01	6.412E-01	3: 4TH
12.40	RE	29.0	.46	4.281E-01	2.097E+00	8.683E-01	6.475E-01	3: 4TH
12.50	RE	29.7	.46	4.318E-01	2.122E+00	8.712E-01	6.534E-01	3: 4TH
12.60	RE	30.3	.46	4.355E-01	2.145E+00	8.740E-01	6.592E-01	3: 4TH
12.70	RE	30.9	.45	4.391E-01	2.166E+00	8.766E-01	6.649E-01	3: 4TH
12.80	RE	31.5	.45	4.425E-01	2.188E+00	8.792E-01	6.702E-01	3: 4TH
12.90	RE	32.2	.45	4.459E-01	2.210E+00	8.817E-01	6.757E-01	3: 4TH
13.00	RE	32.8	.44	4.492E-01	2.233E+00	8.841E-01	6.809E-01	3: 4TH
14.00	RE	39.4	.42	4.787E-01	2.430E+00	9.042E-01	7.266E-01	3: 4TH
15.00	RE	46.3	.40	5.026E-01	2.603E+00	9.190E-01	7.628E-01	3: 4TH
20.00	RE	86.7	.36	5.795E-01	3.266E+00	9.578E-01	8.678E-01	4: 4TH
30.00	RE	206.	.34	6.505E-01	4.126E+00	9.819E-01	9.415E-01	1: 3RD
50.00	RE	745.	.35	7.053E-01	5.175E+00	9.937E-01	9.792E-01	3: 3RD

[a] The column headings are explained in the text. Table entries have been photographed directly from computer output to avoid transcription errors.

Table II
Properties of the Planar and Isotropic Solutions of Eq 15 for the Hard-Core Reference System ($U = 0$) in the Same Format as Table I

B	J	f(0)	L	$\frac{\pi}{4}-\langle\langle\sin\gamma\rangle\rangle$	$\langle\ln f(\theta)\rangle$	$\langle P_2(\cos\theta)\rangle$	$\langle P_4(\cos\theta)\rangle$	Error
8.70	64	.998	.85	2.067E-07	5.042E-05	-3.451E-04	-5.606E-05	-------
8.80	64	.998	.86	2.140E-07	5.045E-05	-3.660E-04	-5.612E-05	-------
8.90	64	.998	.87	2.247E-07	5.050E-05	-3.946E-04	-5.617E-05	-------
9.40	64	.997	.92	3.517E-07	5.108E-05	-6.438E-04	-5.630E-05	-------
9.90	64	.992	.97	1.573E-06	5.704E-05	-1.704E-03	-5.443E-05	-------
10.00	64	.988	.98	3.782E-06	6.505E-05	-2.486E-03	-5.166E-05	-------
10.10	64	.979	.99	9.215E-06	9.541E-05	-4.298E-03	-4.130E-05	-------
10.20	64	.955	.99	4.166E-05	2.603E-04	-9.197E-03	1.388E-05	-------
10.30	RE	.920	.98	1.236F-04	6.363E-04	-1.643E-02	2.054E-04	-------
10.40	RE	.885	.98	3.844F-04	1.486E-03	-2.816E-02	6.462E-04	-------
10.50	RE	.812	.97	7.773E-04	4.040E-03	-3.985E-02	1.316E-03	-------
10.60	RE	.752	.96	1.283E-03	6.706E-03	-5.114E-02	2.183E-03	2: 2ND
10.70	RE	.718	.95	1.683E-03	9.910E-03	-6.194E-02	3.225E-03	1: 2ND
10.80	RE	.675	.94	2.565E-03	1.357E-02	-7.227E-02	4.416E-03	4: 3RD
10.90	RE	.637	.93	3.317E-03	1.766E-02	-8.217E-02	5.739E-03	3: 3RD
11.00	RE	.600	.92	4.127E-03	2.209E-02	-9.164E-02	7.177E-03	2: 3RD
11.10	RE	.567	.91	4.988E-03	2.684E-02	-1.007E-01	8.718E-03	1: 3RD
11.20	RE	.536	.90	5.891E-03	3.189E-02	-1.094E-01	1.035E-02	6: 4TH
11.30	RE	.507	.89	6.831E-03	3.717E-02	-1.179E-01	1.205E-02	4: 4TH
11.40	RE	.480	.88	7.801E-03	4.266E-02	-1.259E-01	1.383E-02	4: 4TH
11.50	RE	.455	.87	8.796E-03	4.836E-02	-1.336E-01	1.566E-02	4: 4TH
11.60	RE	.430	.86	9.812E-03	5.423E-02	-1.411E-01	1.756E-02	3: 4TH
11.70	RE	.408	.85	1.085F-02	6.025E-02	-1.484E-01	1.950E-02	3: 4TH
11.80	RE	.388	.84	1.189E-02	6.640E-02	-1.553E-01	2.147E-02	3: 4TH
11.90	RE	.368	.83	1.295E-02	7.266E-02	-1.620E-01	2.348E-02	3: 4TH
12.00	RE	.350	.82	1.401E-02	7.901E-02	-1.685E-01	2.552E-02	3: 4TH
12.10	RE	.332	.81	1.508E-02	8.546E-02	-1.748E-01	2.758E-02	3: 4TH
12.20	RE	.316	.80	1.615E-02	9.199E-02	-1.809E-01	2.966E-02	3: 4TH
12.30	RE	.301	.79	1.724E-02	9.857E-02	-1.867E-01	3.177E-02	3: 4TH
12.40	RE	.286	.79	1.830E-02	1.052E-01	-1.924E-01	3.388E-02	3: 4TH
12.50	RE	.273	.78	1.937E-02	1.119E-01	-1.979E-01	3.601E-02	3: 4TH
12.60	RE	.260	.77	2.045E-02	1.186E-01	-2.033E-01	3.816E-02	3: 4TH
12.70	RE	.248	.76	2.152E-02	1.253E-01	-2.084E-01	4.029E-02	3: 4TH
12.80	RE	.236	.75	2.258F-02	1.321E-01	-2.136E-01	4.243E-02	3: 4TH
12.90	RE	.225	.74	2.364E-02	1.389E-01	-2.183E-01	4.458E-02	3: 4TH
13.00	RE	.215	.74	2.468E-02	1.457E-01	-2.232E-01	4.673E-02	3: 4TH
14.00	RE	.137	.66	3.470E-02	2.134E-01	-2.639E-01	6.795E-02	3: 4TH
15.00	RE	.089	.60	4.372E-02	2.786E-01	-2.954E-01	8.808E-02	3: 4TH
20.00	RE	.012	.41	7.504E-02	5.486F-01	-3.823E-01	1.668E-01	3: 4TH
30.00	RE	.000	.27	1.032E-01	8.897F-01	-4.405E-01	2.493E-01	3: 4TH
50.00	RE	.000	.19	1.230E-01	1.266E+00	-4.720E-01	3.101E-01	3: 4TH

Now suppose that for $\tilde{f}_i$ and $\hat{f}_i$, any two sets of values "near" f_i, H satisfies the Lipschitz condition

$$\|H(\tilde{f}_i) - H(\hat{f}_i)\| \leq L\|\tilde{f}_i - \hat{f}_i\| \tag{27}$$

with the positive constant $L < 1$. If $f_i^n = H^n(f_i^0)$ is similarly "near" f_i, then

$$\|f_i - f_i^{n+1}\| = \|H(f_i) - H(f_i^n)\| \leq L\|f_i - f_i^n\| \tag{28}$$

and L can be viewed as an error reduction factor for each iteration step. Since

$$\|f_i - f_i^n\| \leq \sum_{r=1}^{\infty}\|f_i^{n+r} - f_i^{n+r-1}\| = \sum_{r=1}^{\infty}\|H^r(f_i^n) - H^r(f_i^{n-1})\| \tag{29}$$

it follows that, when f_i^{n-1} is "near" f_i

$$\|f_i - f_i^n\| \leq \sum_{r=1}^{\infty}L^r\|f_i^n - f_i^{n-1}\| = [L/(1-L)]\|f_i^n - f_i^{n-1}\| \tag{30}$$

Motivated by these results, we defined a numerical estimate of the error to be

$$E_n = [L/(1-L)]\|f_i^n - f_i^{n-1}\|/\|f_i^n\| \tag{31}$$

where L was taken as

$$L = \|H(f_i^{n-1}) - H(f_i^{n-2})\|/\|f_i^{n-1} - f_i^{n-2}\| = \|f_i^n - f_i^{n-1}\|/\|f_i^{n-1} - f_i^{n-2}\| \tag{32}$$

The iteration was stopped when E_n became smaller than a chosen upper bound, τ, which was 1×10^{-5} for the calculations reported in the tables below.

In many of our calculations, the accuracy of the resulting approximations to the derived quantities $\langle\ln f(\theta)\rangle$, $\langle\langle\sin\gamma\rangle\rangle$, $\langle P_2(\cos\theta)\rangle$, and $\langle P_4(\cos\theta)\rangle$ was found to be increased by employing the following standard Richardson extrapolation formula. If Q_J is the approximation to a quantity Q determined from the calculation using a given value of J, a potentially improved approximation is given by

$$Q = (4Q_{2J} - Q_J)/3 \tag{33}$$

A listing of J = "RE" for a given B in Table I or II signifies that all the quantities given were determined using eq 33 with $J = 32$.

Accuracy of the iterative procedure was determined by comparing the results obtained for a sample of B values by alternately taking $J = 16$, 32, and 64, $J_\phi = 1024$ and 2048, $\tau = 1 \times 10^{-5}$ and 1×10^{-6}, and Richardson extrapolation with $J = 16$ and $J = 32$ in eq 33. When obtainable, conservative bounds on the error in the listed values for the four quantities $\langle\ln f(\theta)\rangle$, $\pi/4 - \langle\langle\sin\gamma\rangle\rangle$, $\langle P_2(\cos\theta)\rangle$, and $\langle P_4(\cos\theta)\rangle$ are given in the last column of Tables I and II (e.g., 3:4TH means the error is bounded by 3 in the fourth significant digit).

Results

Empirically, the iteration was found to converge with the notable characteristic that the free energy for successive distribution functions was monotonically decreasing to within round-off error (using 14 significant digits) in all cases examined. This included initial functions that had peaks at both $\theta = 0$ and $\pi/2$, with or without a peak at $\pi/4$, as well as an oscillating initial function. Thus the solutions of eq 15 determined by the iteration always corresponded to local minima of the free energy, which are the solutions of physical interest.

For the hard-core reference system ($U = 0$), we found, in general agreement with the results of Lasher[5] and Kayser and Raveché,[12] that (cf. Tables I and II) (1) all initial choices lead to the isotropic solution for $B < 8.88$, (2) an axial solution is obtained for $B > 8.88$, (3) an isotropic solution is also obtained for $8.88 \leq B < 10.2$, and (4) the isotropic solution is replaced by a planar solution near $B = 10.2$. (A mathematical analysis,[12] discussed in the Appendix, indicates that the exact value of B where the planar solution appears is $32/\pi = 10.186$.) For $B \leq 9.0$ the free energy is always lowest for the isotropic solution and for $B \geq 9.1$ the free energy is always lowest for the axial solution. The free energies of the planar and isotropic solutions are extremely close up to about $B = 10.7$, at which point the free energy of the planar solution

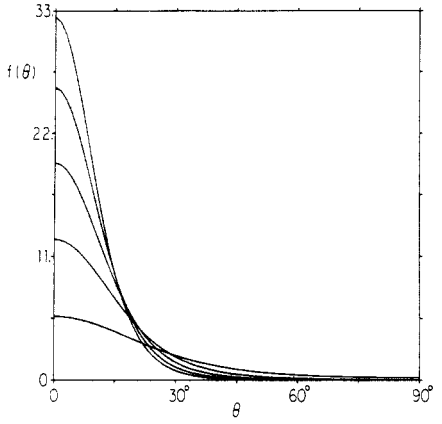

Figure 1. Axial solution of eq 15 for the hard-core reference system ($U = 0$) corresponding, in order of increasing anisotropy, to B = 8.9, 9.7, 10.8, 11.9, and 12.9.

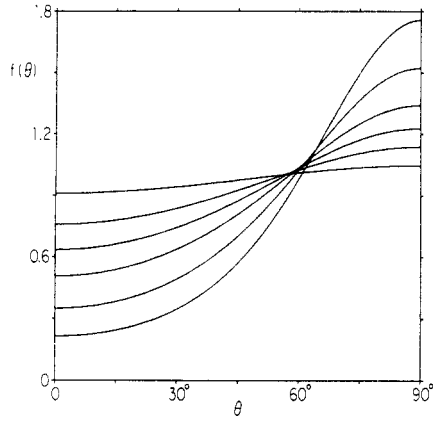

Figure 2. Planar solution of eq 15 for the hard-core reference system ($U = 0$) corresponding, in order of increasing anisotropy, to B = 10.3, 10.6, 10.9, 11.3, 12.0, and 13.0.

becomes distinguishably smaller than that of the isotropic solution. The values of $\pi/4 - \langle\langle \sin \gamma \rangle\rangle$, $\langle \ln f(\theta) \rangle$, $\langle P_2(\cos \theta) \rangle$, and $\langle P_4(\cos \theta) \rangle$ for the axial solution shown in Table I are consistent with those reported by Lasher.[5] The somewhat greater accuracy and significantly wider range of the present results is useful in certain applications (see, e.g., ref 16 and 11).

The constant L (defined in eq 32) which is listed in Tables I and II provides a measure of the "contractiveness" of the iteration near the converged distribution (as indicated in eq 28). Hence, as L decreases, the convergence of the iterative algorithm becomes more rapid. From a practical standpoint, the convergence is reasonably rapid for axial solutions for $B \geq 8.9$ and for planar solutions for $B \geq 10.3$ and becomes very rapid as B increases from these values. One can also observe that the value of B (very close to 8.88) at which the axial solution no longer exists is presaged by the approach of L to 1, as is the value of B (near 10.2) at which the planar solution appears.

In an addition test of the iterative algorithm, long-range interparticle interactions were introduced in the form

$$\rho U(\gamma_{12})/kT = -\sum_{m=2,2}^{4} C_m P_m(\cos \gamma_{12}) \qquad (34)$$

Calculations were performed for B = 8.7 and 9.4 with axial starting values and for B = 10.0 with isotropic starting values for a number of values of C_2 and C_4. The algorithm monotonically decreased the free energy and converged as before. The qualitative effect on the distribution function of increasing C_2 and C_4 for a given value of B was, as expected, roughly equivalent to increasing B for given values of C_2 and C_4.

Conclusions

The nonlinear integral equation for the orientation distribution function of rodlike particles has a form that lends itself to iterative solution. Iteration in this manner can be analytically demonstrated to move in a direction of decreasing free energy. In addition, we find that, for the range of problems considered, the iteration converges with remarkable efficiency (i.e., with generally small Lipschitz constants, cf. Tables I and II). The method provides highly accurate axial and planar solutions for monodisperse hard-core particles with a wide range of aspect ratios and densities. The approach is sufficiently general that it can be expected to apply to other particle populations with more complicated properties.

Acknowledgment. This work was supported by a grant-in-aid from the American Heart Association (with funds contributed in part by the Massachusetts affiliate), by the Naval Surface Weapons Center Independent Research Fund, and by National Institutes of Health Biomedical Research Support Grant RR05381. We are also grateful to a reviewer for calling our attention to a relevant paper.

Appendix. The Planar Branch Point

We outline, in terms of our notation, a finite dimensional, and therefore more accessible, version of the bifurcation analysis carried out by Kayser and Raveché.[12] The value of B at which the planar solution appears can be determined by expanding $f(\Omega)$ as in eq 6 and $W(\gamma)$ as in eq 8 (with the coefficients w_m given by eq 13), thus reducing the free energy in eq 9 to a function $F(\eta_2, \eta_4, ..., \eta_M)$. A necessary condition for $\{\eta_m\}$ to determine a local extremum of F is that $\partial F/\partial \eta_m = 0$ for $m = 2, 4, ..., M$. Local uniqueness of a solution $\{\eta_m\}$ of the latter set of equations is guaranteed by the nonsingularity at $\{\eta_m\}$ of the matrix of second partial derivatives $H_{ij} = \partial^2 F/\partial \eta_{2i} \partial \eta_{2j}$.[17] For the isotropic solution ($\eta_m = 0$ for all m), H is easily seen to be the diagonal matrix with $H_{ii} = (4i + 1) + Bw_{2i}$, $i = 1, 2, ..., M/2$. For the hard-core reference system ($U = 0$) the values of w_m are[13] $w_0 = \pi/4$, $w_2 = -5\pi/32$, $w_4 = -9\pi/256$, and $w_{m+2} = w_m(2m^3 + 5m^2 - 2m - 5)/(2m^3 + 13m^2 + 22m + 8)$, for $m = 4, 6, ...$ Hence, the first value of B for which the isotropic solution could fail to be locally unique is $B = 32/\pi$. Since exactly one eigenvalue of H changes sign at $B = 32/\pi$, there must indeed be a branch of nonisotropic solutions of $\partial F/\partial \eta_m = 0$ off of the isotropic solution at $B = 32/\pi$.[18,19] For $B > 32/\pi$, the isotropic solution and all solutions that subsequently branch from it, as successive eigenvalues of H change sign, are saddle points of F.

References and Notes

(1) Chandler, D.; Weeks, J. D.; Andersen, H. C. *Science (Washington, D.C.)* **1983**, *220*, 787–794.
(2) Gelbart, W. M.; Baron, B. A. *J. Chem. Phys.* **1977**, *66*, 207–213. Cotter, M. A. *Ibid.* **1977**, *66*, 4710–4711.
(3) Cotter, M. A. *J. Chem. Phys.* **1977**, *67*, 4268–4270.
(4) Gelbart, W. M.; Gelbart, A. *Mol. Phys.* **1977**, *33*, 1387–1398.
(5) Lasher, G. *J. Chem. Phys.* **1970**, *53*, 4141–4146.
(6) Onsager, L. *Ann. N. Y. Acad. Sci.* **1949**, *51*, 627–659.
(7) Baron, B. A.; Gelbart, W. M. *J. Chem. Phys.* **1977**, *67*, 5795–5801.
(8) Alben, R. *Mol. Cryst. Liq. Cryst.* **1971**, *13*, 193–231.
(9) Cotter, M. A. *J. Chem. Phys.* **1977**, *66*, 1098–1106.
(10) Morse, P. M.; Feshbach, M. "Methods of Theoretical Physics"; McGraw-Hill: New York, 1953; p 1274.
(11) Kubo, K.; Ogino, K. *Mol. Cryst. Liq. Cryst.* **1979**, *53*, 207–228.
(12) Kayser, R. F., Jr.; Raveché, H. J. *Phys. Rev. A* **1978**, *17*, 2067–2072.
(13) Gradshteyn, I. S.; Ryzhik, I. M. "Table of Integrals, Series and Products"; Academic Press: New York, 1980; p 798.
(14) Cotter, M. A.; Wacker, D. C. *Phys. Rev. A* **1978**, *18*, 2669–2675.

(15) Berger, A. E., submitted for publication.
(16) Cotter, M. A. *Phys. Rev. A* **1974**, *10*, 625–636.
(17) Sattinger, D. H. *Bull. Am. Math. Soc.* **1980**, *3*, 779–819. (See theorem on page 782.)
(18) Sattinger, D. H. "Topics in Stability and Bifurcation Theory"; Springer-Verlag: New York, 1973; pp 141–144.
(19) Crandall, M. G.; Rabinowitz, P. H. *Arch. Rational Mech. Anal.* **1973**, *52*, 161–180.

Statistical Analysis of Quasi-Elastic Light Scattering Data

G. J. Wei and Victor A. Bloomfield*

Department of Biochemistry, University of Minnesota, St. Paul, Minnesota 55108.
Received November 18, 1983

ABSTRACT: We often observe a linear correlation between the first and the second cumulants when analyzing autocorrelation functions obtained in quasi-elastic light scattering (QLS). For time-invariant samples, this is explained by a theory based on random noise effects. The theory is supported by evidence from computer simulation and from experimental QLS study of polystyrene latex spheres. Using these results, we propose a method for reducing scatter of QLS data from a reacting system and illustrate it by a simulated example.

Introduction

Quasi-elastic light scattering (QLS) has become a convenient and reliable tool for obtaining hydrodynamic properties of macromolecules.[1,2] With the cumulant method of data analysis,[3] one gets a z-averaged diffusion coefficient from the first cumulant and a relative variance or "quality factor" from the second cumulant, which reflects the width of the size distribution of the sample.

In our routine QLS measurements of various types of samples, we often observe a pattern in the variation of the diffusion coefficient D and the quality factor $Q = \langle (D - \langle D \rangle)^2 \rangle / \langle D \rangle^2$. For a given sample under identical experimental conditions, repeated measurements show that variations in D and Q are linearly correlated.

In this paper we show how this observation can be explained by a statistical theory of the effect of random noise on the least-squares fitting process. Using this experimental observation and the theoretical explanation, we suggest a method to improve data from QLS measurements on time-dependent samples.

Theory

Let $\epsilon(0,\sigma^2)$ represent Gaussian random numbers with a mean value of zero and a standard deviation of σ. Then, for a "noise-infected" quadratic function

$$f(x) = b_0 + b_1 x + b_2 x^2 + \epsilon(0,\sigma^2) \tag{1}$$

the correlation among the expected values β_0, β_1, and β_2 (corresponding to b_0, b_1, and b_2), obtained from least-squares fitting, is given by the Variance Matrix,[4] **V**:

$$\mathbf{V} = \begin{pmatrix} v_{11} & v_{12} & v_{13} \\ v_{21} & v_{22} & v_{23} \\ v_{31} & v_{32} & v_{33} \end{pmatrix} = \sigma^2(\mathbf{x}^T\mathbf{x})^{-1} \tag{2}$$

where

$$\mathbf{x} = \begin{pmatrix} 1 & x_1 & x_1^2 \\ 1 & x_2 & x_2^2 \\ \cdot & \cdot & \cdot \\ \cdot & \cdot & \cdot \\ \cdot & \cdot & \cdot \\ 1 & x_n & x_n^2 \end{pmatrix} \tag{3a}$$

$$\mathbf{x}^T = \begin{pmatrix} 1 & 1 & \dots & 1 \\ x_1 & x_2 & \dots & x_n \\ x_1^2 & x_2^2 & \dots & x_n^2 \end{pmatrix} \tag{3b}$$

and x_i is the ith data point.

The variance of each fitted parameter is given by the corresponding diagonal element of **V**. The off-diagonal elements indicate the correlations between fitted parameters. If, for example, β_2 is plotted against β_1 for a large number of fits, the least-squares slope for the plot would be V_{23}/V_{22}.

In light scattering experiments, the noise appears in the exponential function, while the least-squares fitting is usually carried out after taking the logarithm. The theory needs to be modified as follows:

$$f'(x) = \ln [\exp(b_0 + b_1 x + b_2 x^2) + \epsilon] \tag{4}$$

This may be expanded about $\epsilon = 0$ as

$$f'(x) = (b_0 + b_1 x + b_2 x^2) + \epsilon \exp[-(b_0 + b_1 x + b_2 x^2)] + \mathcal{O}(\epsilon^2) \tag{5}$$

If terms of higher order than ϵ can be ignored, the Variance Matrix for the new set of fitted parameters (β_0', β_1', β_2') would be (see Appendix)

$$\mathbf{V}' = \begin{pmatrix} V_{11}' & V_{12}' & V_{13}' \\ V_{21}' & V_{22}' & V_{23}' \\ V_{31}' & V_{32}' & V_{33}' \end{pmatrix} = \sigma^2(\mathbf{x}^T\mathbf{x})^{-1}(\mathbf{x}^T\mathbf{w}\mathbf{x})(\mathbf{x}^T\mathbf{x})^{-1} \tag{6}$$

where **w** is an $n \times n$ diagonal matrix with the diagonal elements

$$w_{ii} = \exp[-(b_0 + b_1 x_i + b_2 x_i^2)] \tag{7}$$

Again a plot of β_2' vs. β_1' should yield a slope, β, given by V_{23}'/V_{22}'.

In cumulant analysis, the logarithm of the photocurrent autocorrelation function, $C(t)$, is fitted to a quadratic equation:

$$y(t) = \tfrac{1}{2} \ln C(t) = a - bt + ct^2/2 \tag{8}$$

where $b = q^2\langle D \rangle$, $c = q^4\langle (D - \langle D \rangle)^2 \rangle$, q is the scattering wavevector $= (4\pi\tilde{n}/\lambda) \sin(\theta/2)$, λ is the wavelength of laser light, $\tilde{n}$ is the refractive index of the medium, θ is the scattering angle, and Q is the quality factor $= \langle (D - \langle D \rangle)^2 \rangle / \langle D \rangle^2 = c/b^2$.

Let b', c', and Q' be the "true" values of b, c, and Q, respectively, and $\Delta b = b - b'$, $\Delta c = c - c'$, and $\Delta Q = Q - Q'$ the corresponding differences. We have used the term "true" value to indicate the value that one would obtain in the absence of random noise. It may include systematic

0024-9297/84/2217-1723$01.50/0